

Spatial and temporal variation in dissolved organic matter in urban streams in metropolitan Boston, Massachusetts (USA)

Annika M. Quick^{1,7}, Allison H. Roy^{2,8}, Rebecca L. Hale^{3,9}, Kristina G. Hopkins^{4,10}, Shuo Chen^{3,5,11}, and Liz D. Ortiz Muñoz^{6,12}

¹Earth and Environmental Sciences Department, Virginia Wesleyan University, Virginia Beach, Virginia, USA

²United States Geological Survey, Massachusetts Cooperative Fish and Wildlife Research Unit, University of Massachusetts Amherst, Amherst, Massachusetts, USA

³Smithsonian Environmental Research Center, Edgewater, Maryland, USA

⁴United States Geological Survey, Washington Water Science Center, Tacoma, Washington, USA

⁵Odum School of Ecology, University of Georgia, Athens, Georgia, USA

⁶Institute of Environment and Department of Biological Sciences, Florida International University, Miami, Florida, USA

Abstract: Urban riverine systems are heterogeneous, and the substantial variability in impervious cover, riparian cover, wetlands, and wastewater and stormwater infrastructure affect sources and transport of dissolved organic matter (DOM), of which dissolved organic C (DOC) is a substantial component. An understanding of the quantity, bioavailability, and timing of DOM inputs (a key energy source for food webs and a component of nutrient cycling) to streams within cities can help to better evaluate drivers of DOM variability. We sampled 100 stream sites in the greater Boston (Massachusetts, USA) area spanning a range of land cover, riparian vegetation, stream size, housing and infrastructure age, and sociodemographic characteristics. Water samples collected during 4 seasonal synoptic events in 2021 and 2022 were analyzed for DOC concentration and DOM characteristics (using fluorescence excitation–emission matrices and absorbance spectra). Temporally, we observed more-autochthonous DOM and lower DOC concentrations in the summer, possibly due to low precipitation and streamflow disconnecting streams from humic wetland and soil C sources. Consistent with other studies, we observed that more-urbanized streams had DOM that was less humic and more autotrophic. Higher wetland cover was associated with more-humic, higher-molecular-weight DOM and was the strongest predictor of DOM characteristics, suggesting that managers should consider the impacts of development on DOM, stream ecological functions, and CO₂ emissions. Interestingly, except during the very dry summer, sites downstream of combined sewer outfalls showed distinctly higher concentrations of protein-like DOM, suggesting the influence of sewage overflows and highlighting the potential for monitoring wastewater contamination using protein-like DOM. Although sociodemographic variables were not strong predictors of DOM composition, we observed a possible association between lower-income areas with less canopy cover and more-autochthonous DOM and between areas with older housing, more canopy cover, and more-humic DOM. These patterns suggest that equitable repair of wastewater infrastructure and restoration of riparian vegetation is needed. **Key words:** urban hydrology, dissolved organic carbon, combined sewer overflows, impervious cover, wetlands, stream metabolism, PARAFAC, wastewater, stormwater, riparian vegetation, fluorescence, sociodemographics

INTRODUCTION

Urban development alters the physical structure of river and stream ecosystems through increases in the surface area of impervious cover, more frequent channelization (Hancock

2002, Hasenmueller and Robinson 2016) and stream burial (Roy et al. 2009, Napieralski et al. 2015, Forgrave et al. 2022), and removal of wetlands and natural riparian buffers

Email addresses: ⁷aquick@vwu.edu; ⁸aroy@eco.umass.edu; ⁹haler@si.edu; ¹⁰khopkins@usgs.gov; ¹¹schen83@crimson.ua.edu; ¹²lorti080@fiu.edu

ORCID iDs: A. Quick, <https://orcid.org/0000-0002-2745-7831>; A. Roy, <https://orcid.org/0000-0002-8080-2729>; R. Hale, <https://orcid.org/0000-0002-3552-3691>; K. Hopkins, <https://orcid.org/0000-0003-1699-9384>; S. Chen, <https://orcid.org/0000-0002-7243-0136>; L. Ortiz Muñoz, <https://orcid.org/0000-0002-2345-4430>.

Received 15 June 2024; Accepted 8 May 2025; Published online 27 August 2025; Associate Editor, Nathan J. Smucker

Freshwater Science, volume 44, number 4, December 2025. © 2025 The Society for Freshwater Science. All rights reserved. Published by The University of Chicago Press for the Society for Freshwater Science. <https://doi.org/10.1086/736917>

(Johnson et al. 2020, Birch et al. 2022). These physical impacts strongly influence stream hydrology and biogeochemistry, which has myriad impacts on stream ecosystem structure and function, sometimes referred to as the Urban Stream Syndrome (Walsh et al. 2005). In particular, urbanization can shift dissolved organic matter (DOM) sources and bioavailability (e.g., Hosen et al. 2014, Parr et al. 2015, Roebuck et al. 2020, Coble et al. 2022), which can have cascading ecosystem effects because of the role of organic matter as an energy source (Allan et al. 2021) and links to nutrient processing (Kaushal et al. 2014, Flint and McDowell 2015, Graeber et al. 2021). Urban watershed and ecosystem management can be improved with a mechanistic understanding of how various aspects of urbanization shape ecosystem structure and function, including controls on DOM.

Many studies have examined how human activities influence DOM inputs, as well as instream processing and production of organic matter. Generally, urbanization is associated with a shift from terrestrial and humic organic matter to more-autochthonous organic matter (Hosen et al. 2014, Parr et al. 2015, Coble et al. 2022), especially as streams are channelized and decoupled from riparian zones (Roebuck et al. 2020). Novel urban anthropogenic sources include inputs of C and other nutrients from human infrastructure (e.g., wastewater treatment plants, leaky sewers, septic systems, storm drains; Griffith et al. 2009, Regnier et al. 2013), landscaping activities (e.g., fertilizer runoff, grass clippings), and potentially from plastic litter that leaches DOM (Egea et al. 2024). Activities such as street sweeping can also alter the inputs of leaf-litter leachate downstream of gutters (Bratt et al. 2017). Infrastructure changes designed to alter hydrologic flow in urban areas (e.g., channelization, stormwater conveyances, stream burial) generally lead to higher and more rapid flows (e.g., Bhaskar et al. 2020) that are disconnected from soils and hyporheic zones, altering the relative contributions of allochthonous DOM, such as leaf-litter leachate and soil organic matter, and the residence time for sorption or degradation of organic matter (Xenopoulos et al. 2021).

Urbanization also affects light availability (increased through removal of riparian vegetation or decreased through stream burial), which can affect autochthonous C sources (Arango et al. 2017). Autochthonous DOM is produced in the stream by algae, microbes, or phytoplankton (Sondergaard and Middelboe 1995, McKnight et al. 2001, Mostofa et al. 2013). The shift from allochthonous to autochthonous DOM with urbanization, where canopy cover has been reduced and there are elevated anthropogenic nutrient inputs, may be due to higher instream primary productivity (Hosen et al. 2014, Parr et al. 2015). DOM is also increasingly labile in urban streams, with more protein-like fractions in streams with more impervious cover (Hosen et al. 2014, Kaushal et al. 2014, Smith et al. 2021). The increase in protein-like DOM may be due to more wastewater leakage in developed areas with more impervious cover or more light availability for growth of algae and mi-

crobes in streams where riparian vegetation has been removed (Petrone et al. 2011, Eckard et al. 2017, Batista-Andrade et al. 2024).

Although there are emerging predictable patterns of DOM with urbanization, DOM is also likely to vary within cities. As a result of variation in the type of development and infrastructure, vegetative cover, and social demographics, urbanization could have variable impacts on DOM for individual streams (Xenopoulos et al. 2021). For example, infrastructure age and type, which often varies between city centers and younger suburbs, strongly influences potential contamination from leaky sewer pipes or combined sewer overflow (CSO) events (Kaushal and Belt 2012, Parr et al. 2016, Hopkins and Bain 2018). Varying social demographics within a city may also influence past and present investment in infrastructure and vegetation (e.g., Locke et al. 2021, Napieralski et al. 2024), with important consequences for DOM inputs and processing. For example, lower investment in repairing infrastructure may increase the likelihood of leakage from aging wastewater pipes. An understanding of drivers of within-city variability in DOM may reveal important mechanisms of urban impacts on streamwater quality and suggest management interventions that minimize alteration from natural conditions.

The magnitude and direction of human impacts on stream DOM dynamics also varies with seasonal and hydrologic conditions. For example, across a range of forested to developed catchments, DOM was unrelated to land use during periods of low flow, presumably because of disconnection from terrestrial sources (Coble et al. 2022). DOM characteristics may also change with flow conditions. During high flows, less processing of labile DOM in natural systems may result in DOM with higher bioavailability (Raymond et al. 2016, Chen et al. 2019), or storm events may result in an increased contribution of humic DOM from terrestrial sources (Inamdar et al. 2011). In urban stream systems, high flows can shape DOM sources and characteristics because of the activation of new flow paths, such as stormwater runoff and groundwater connectivity (Smith et al. 2021). On a global scale, prolonged dry periods or increased flooding caused by anthropogenic climate change may indirectly influence the characteristics of stream DOM (Xenopoulos et al. 2021). Studies that show both minor seasonal effects (Coble et al. 2022) and substantial and varying seasonal effects (e.g., Hosen et al. 2014, Kaushal et al. 2014, Arango et al. 2017, Smith et al. 2021) suggest that temporal variability in DOM sources can affect how urban sources of DOM change under different flow conditions.

In this study, we investigated spatial and temporal drivers of streamwater DOM variability in the Boston (Massachusetts, USA) metropolitan area. Specifically, we addressed the following questions: How do the quantity and characteristics of urban stream DOM vary 1) temporally among 4 sampling seasons with different hydrology and phenology conditions and 2) spatially within a city where watersheds vary in physical and sociodemographic characteristics? We hypothesized

that temporal variation would be tied to humic leaf-litter inputs in the autumn. Spatially, we hypothesized that more-urbanized watersheds, as indicated by impervious cover, would be characterized by more-autotrophic DOM and lower dissolved organic C (DOC) concentrations (in line with previous research such as Hosen et al. 2014, Parr et al. 2015, Coble et al. 2022) and that streams downstream of CSOs would have wastewater signatures. We also hypothesized that sociodemographic characteristics would influence DOM characteristics in the following 2 ways: watersheds with older infrastructure would contribute more-humic DOM, and lower-income areas with less canopy cover would have a larger contribution of autotrophic DOM. The results of this study provide insight into mechanisms of urban impacts on riverine DOM and may guide within-city management decisions regarding development of wetland areas and equitable maintenance of infrastructure and riparian restoration, particularly because many cities are undergoing shifts in water management paradigms necessitated by aging infrastructure and expanding development (Parr et al. 2016).

METHODS

To elucidate drivers under various urban and hydrometeorological conditions, we sampled 100 urban stream sites during 4 synoptic events over 1 y (early autumn, late autumn, spring, and summer) and tested for differences in the sources, quantity, and characteristics of riverine DOM, which are relevant to many biogeochemical processes, such as denitrification (Bernhardt and Likens 2002), light penetration and photosynthesis (Mostofa et al. 2013), and the transport and release of contaminants (Findlay 2006, Kaushal et al. 2018). We used analysis of variance (ANOVA) to assess seasonal differences between both DOM optical properties and parallel factor analysis (PARAFAC) modeled components and multiple linear regression modeling to assess relationships between watershed characteristics and DOM.

Study area

The study area included the greater Boston metropolitan area (42.0–42.6°N, 71.0–71.6°W) and encompassed the watersheds of 3 major rivers: the Charles River, the Mystic River, and the Neponset River (Fig. 1A). The combined watershed area is ~1300 km² and has a population of nearly 5 million people (USCB 2010). The area has a temperate climate and receives an average of 111 cm of annual precipitation, typically without distinct wet and dry seasons (NOAA 2024; Table S1).

Rivers and streams in the Boston area have experienced >400 y of urban influence, including construction of canals and dams beginning in the 1600s and infilling of marshes beginning in the 1700s. In Massachusetts, statewide, ~28% of wetlands have been lost since the 1780s, and based on aerial imagery from 1990 to 2012, commercial and residential development continues to cause loss of wetlands (NAWM

2015, Rhodes et al. 2019). Beginning in the mid-1830s, combined sewers carried waste and stormwater directly into the rivers. The first wastewater treatment plants were constructed in the mid-1900s. Since 2000, except for scattered septic systems (mostly in the upper Neponset watershed), nearly all wastewater has been routed to the Deer Island Treatment Plant in Boston Harbor (USEPA 2023b, BWSC 2024). The current sewer infrastructure includes both combined (stormwater and wastewater) and separated systems, with stormwater pipes routing stormwater to streams and CSOs releasing wastewater into streams and rivers during heavy precipitation (Fig. 1C, D). Efforts to remove illicit discharges, close CSO outfalls, and separate combined sewer systems began in the late 1980s and 1990s. Since 1987, CSO discharge has been eliminated from ~40 of 84 outfalls (MWRA 2024b); however, millions of gallons of untreated wastewater are released every year into these watersheds, amounting to hundreds of millions of gallons in wet years (MWRA 2022, Mystic River Watershed Association 2022). As such, contamination from aging sewer pipes and CSOs is a major concern in this area.

Sampling locations

To represent the range of urban conditions in the greater Boston area, 100 stream and river sites were selected for synoptic sampling, with sites distributed among the 3 watersheds based roughly on the watershed size: 40 sites in the Charles River watershed (809 km²), 35 sites in the Neponset River watershed (311 km²), and 25 sites in the Mystic River watershed (197 km²). To reflect a range of streams from headwaters to large river orders, 26 sites were located in the main stems of the 3 rivers (Charles, Neponset, and Mystic), and 74 sites were located in tributaries to those rivers. Drainage areas ranged from 0.3 to 800 km². Watersheds for the sampling locations reflected a range of impervious cover (0–88%), wetland cover (0–33%), population density (0–8120 people/km²), median housing age (12.1–70.8 y) as a proxy for infrastructure age, and other physical and sociodemographic characteristics (see Table S2).

Watershed characteristics

We delineated watersheds for each of the synoptic sites with a 1/3 arc second (~10 m) digital elevation model (DEM) obtained from the United States Geological Survey National Map (USGS 2021b). We used the least cost path tool in the *whitebox* package (version 2.4.0; Lindsay 2016, Wu and Brown 2022) for R statistical software (version 4.4.1; R Project for Statistical Computing, Vienna, Austria) in the RStudio® Integrated Development Environment for R (version 2024.12.1; Posit® Software, PBC, Boston, Massachusetts) to delineate watershed by breach depressions in the DEM. We then used the breached and filled DEM to generate an 8-direction flow pointer and flow accumulation raster. We snapped the synoptic sampling locations to the flow accumulation raster by

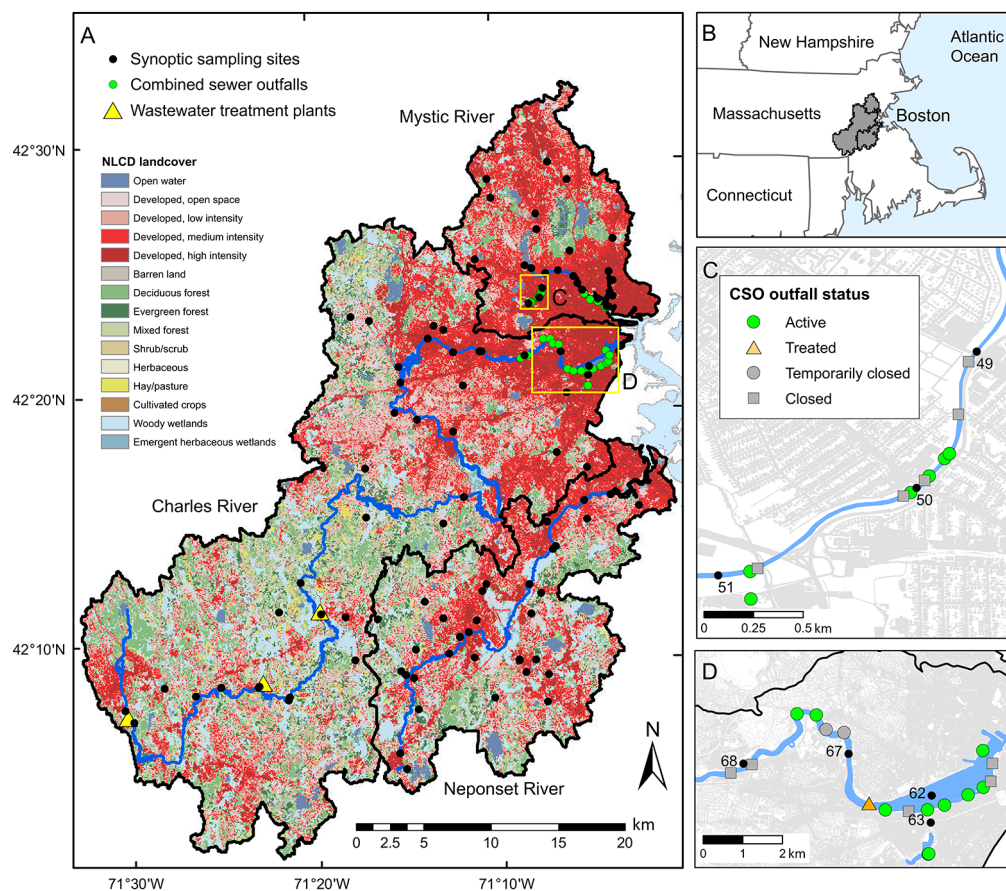


Figure 1. Study area showing land cover (from 2021 National Land Cover Database [NLCD]; Dewitz 2023) and the synoptic sampling sites ($n = 100$) in the greater Boston, Massachusetts, USA, area (A). Green circles show the locations of active and closed combined sewer overflow (CSO) outfalls that are upstream of sampling sites. Portions of the study area that include CSO outfalls are outlined by boxes C and D. The 3 main watersheds, outlined in thick black lines, are from north to south: Mystic River watershed, Charles River watershed, and Neponset River watershed. These 3 watersheds are shown on the inset map of the northeastern United States (B). CSO outfalls along Alewife Brook, a tributary of the Mystic River (C). CSO outfalls along the Muddy River (tributary on the south side) and the Charles River (D). The gray shading in the background of panels C and D shows impervious cover, and numbers indicate site numbers.

hand to ensure proper placement along the flow path. We then used the unnested basins tool to generate the upstream drainage area for each synoptic sampling location.

We completed all watershed characteristic calculations in ArcGIS® Pro (version 3.1.3; Environmental Systems Research Institute [ESRI®], Redlands, California). We characterized land cover (wetland cover, forest cover) and impervious cover with the 2021 National Land Cover Dataset (NLCD; <https://doi.org/10.5066/P9JZ7AO3>; Dewitz 2023). Tree canopy cover was characterized using the NLCD 2021 United States Forest Service Tree Canopy Cover data (<https://www.mrlc.gov/data/nlcd-2021-usfs-tree-canopy-cover-conus>; USGS 2021a). We calculated annual precipitation, minimum and maximum air temperature, and mean elevation in each watershed from a 4-km-resolution DEM obtained from the parameter-elevation regressions on independent slopes model (PRISM Climate Group 2023; <https://prism.oregonstate.edu/>), which was available for all of the cities included in a larger study of DOC in urban rivers (Hopkins et al. 2024, Roy et al. 2025, LDOM, RLH, and SH, unpublished data). The density of CSOs (no./km²) was determined from CSO outfalls reported within the United States Environmental Protection Agency (EPA) Enforcement and Compliance History Online (<https://echo.epa.gov/>; USEPA 2014). We calculated the volume of CSO flows in the 30 d prior to sampling based on CSO reports from local reporting agencies (CDPW 2024, City of Somerville 2024, MEOEEA 2024, MWRA 2024a). We calculated drainage density for each watershed with the National Hydrography Plus High Resolution National Release 1 (<https://www.usgs.gov/national-hydrography/nhdplus-high-resolution>) using flow types coded as stream/river, canal, and artificial path (USGS 2023).

To investigate the potential role of sociodemographic variables in stream DOM, we calculated variables potentially

to investigate the potential role of sociodemographic variables in stream DOM, we calculated variables potentially

related to the age, condition, and maintenance of infrastructure and to canopy cover for watersheds using data from EPA and census records. Low-income population (%) and people of color (%) were summarized from the EPA's Environmental Justice Screening and Mapping Tool (EJ Screen; <https://doi.org/10.7910/DVN/RLR5AX>) at the block group level (USEPA 2023a). We estimated sociodemographic variables for median household income (in USD) and housing density (housing units/km²) from tract-level data from the 2010 United States Census American Community Survey, downloaded using the *tidycensus* package (version 1.7.1; Walker and Herman 2025) in R and joined to United States Census Topologically Integrated Geographic Encoding and Referencing System (TIGER)/Line[®] tract boundaries (<https://www.census.gov/geographies/mapping-files/time-series/geo/tiger-line-file.html>). We estimated % owner-occupied housing from block-level census data (USCB 2010). Other studies have found that street sweeping influences the input of leaf-litter leachate to urban streams (Bratt et al. 2017), and we estimated street-sweeping frequency for each watershed as low, medium, or high based on sweeping frequencies reported by municipalities within the watershed boundaries.

Watershed boundaries and watershed characteristics are provided in Hopkins et al. (2024).

Field methods

All 100 sites were sampled over a 1-to-2-wk period (7–13 d) to capture a snapshot of stream biogeochemistry at 4 times over 1 y with different vegetative and hydrological conditions: September 2021 (late summer of a wet year), November 2021 (during leaf fall), April 2022 (during green up), and July 2022 (full canopy cover, midsummer). Because of the large number of sampling locations and frequent rainfall during the first 3 synoptic event seasons, it was impractical to collect all samples during baseflow conditions, although no samples were collected during active rainfall (Fig. 2). Although discharge hydrographs were only available at a few sites, we assume that some of the samples were inevitably collected during rising or falling discharge, which limits our interpretation of seasonal trends as described in the Discussion section. Several CSO events occurred during the year, particularly in 2021 (Fig. 2B), though these overflow events were only upstream of a few of the sampling sites (see Fig. 1). There were dry conditions during the final sampling event in

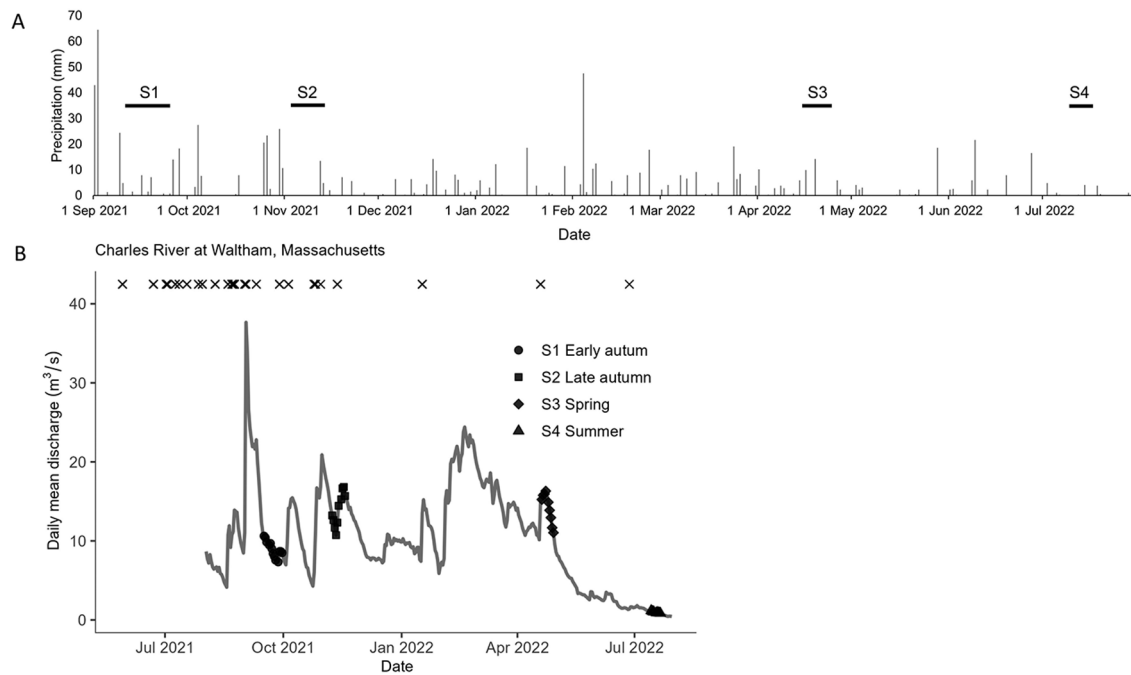


Figure 2. Daily precipitation at Boston Logan Airport from September 2021 to July 2022 (NOAA 2024), with horizontal bars showing the timing of the 4 synoptic sampling events (S1 through S4) (A). Daily mean discharge at the United States Geological Survey (USGS) stream gauge located on the Charles River at Waltham, Massachusetts, USA (USGS station 01104500, watershed area = 645 km²), from August 2021 through July 2022 (<https://waterdata.usgs.gov/monitoring-location/01104500>) (B). The dates for each of the 4 synoptic sampling events (S1 through S4) are overlain on the hydrograph with symbols. Combined sewer overflow events that occurred in the greater Boston area (not upstream of this USGS station) are shown along the top as × symbols. This hydrograph should not be interpreted as showing flow conditions (stormflow or baseflow) at individual sampling sites, which may look very different (an example hydrograph at a smaller stream during the same time period is shown in Fig. S6).

July 2022, and 3 of the streams could not be sampled because the channels were dry.

During synoptic sampling, we measured physicochemical stream parameters (pH ± 0.2 units, water temperature $\pm 0.2^\circ\text{C}$, dissolved O_2 [DO] ± 0.1 mg/L, specific conductivity ± 0.002 mS/cm) with a ProDSS multiparameter digital water quality meter (YSI 626870; Yellow Springs Instruments, Yellow Springs, Ohio) and collected water samples at each site during daylight hours. We collected water samples from the thalweg with a swing sampler (model B01366; Nasco Sampling LLC, Fort Atkinson, Wisconsin) or Van Dorn-type bridge sampler (model 031868; Wildco[®], Yulee, Florida). For large rivers where we could not sample from a bridge, we sampled

from the bank, using a swing sampler to sample as far as possible toward the center of the river (~ 4 m). Sampling methods at specific sites are published in Quick et al. (2025). Collection devices were triple rinsed with site water prior to sample collection. Using new, triple-rinsed plastic 60-mL syringes, we filtered sample water through pre-combusted and pre-weighed 0.7- μm glass fiber filters (catalog no. AP4004700; MilliporeSigma[®], Burlington, Massachusetts) and then filtered the samples through 0.2- μm polyethersulfone disposable syringe filters (catalog no. 9915-2502; Cytiva[®], Marlborough, Massachusetts) for analysis of DOC. We collected samples for DOC concentration and fluorescent DOM (fDOM) in new, sample-water-rinsed, 60-mL amber high-density

Table 1. Dissolved organic matter (DOM) optical properties, including calculation methods and references.

Abbreviation	Parameter	Calculation	Description	References
BIX	Biological index	The ratio of emission intensity at 380 nm divided by 430 nm at excitation 310 nm	An indicator of autotrophic productivity. High values (>1) correspond to recently produced DOM of autochthonous origin. Ranges from 0.6 (low productivity) to >1 (high productivity).	(Fellman et al. 2010, Hansen et al. 2016)
HIX	Humification index	The area under the emission spectra at 435–480 nm divided by the peak area at 300–345 nm and 435–480 nm, at excitation 254 nm	An indicator of humic substance content or extent of humification. Higher values indicate an increasing degree of humification. Note: The Ohno (2002) method corrects for secondary inner-filter effects, is concentration independent, and ranges between 0 and 1. Values range from 0 (less humic) to 1 (more humic).	(Ohno 2002)
FI	Fluorescence index	Calculated as emission intensity (470 nm/520 nm) at 370 nm excitation	Ratio ~ 1.2 reflects terrestrially derived fulvic acids, ~ 1.8 reflects microbially derived fulvic acids.	(Cory and McKnight 2005, Cory et al. 2010)
SR	Slope ratio	Best-fit slope of $\ln(\text{absorbance})$ at 275–295 nm divided by best-fit slope of $\ln(\text{absorbance})$ at 250–400 nm	Negatively correlated with mean molecular weight. Very sensitive to photobleaching, which increases SR values. Values range from 0.7 (blackwater) to 10 (open ocean).	(Helms et al. 2008)
E2:E3	Ratio of absorbance at 250 nm to absorbance at 365 nm	Ratio of absorbance at 250 nm to absorbance at 365 nm	Negatively correlated with molecular weight and aromaticity.	(De Haan and De Boer 1987, Li and Hur 2017)
$S_{275-295}$	–	Nonlinear slope of absorbance at 275–295 nm	Proxy for DOM molecular weight. Very sensitive to photobleaching.	(Helms et al. 2008)
$S_{350-400}$	–	Nonlinear slope of absorbance at 350–400 nm	Typically, higher $S_{350-400}$ values indicate low molecular weight material, decreasing aromaticity, or both.	(Blough and Del Vecchio 2002, Helms et al. 2008)

polyethylene bottles. We collected duplicate samples at 10% of the sites, and we used the same filtration procedures as the experimental samples to create field blanks of ultra-pure Milli-Q (MilliporeSigma) water daily. Field samples for DOC and fDOM were shipped on ice to Florida International University, Miami, Florida, where they were refrigerated (4°C) until analysis (mean holding time = 43 d).

Laboratory methods

We analyzed filtered water samples for DOC concentration using a total organic C analyzer (Shimadzu TOC-V; Shimadzu®, Kyoto, Japan), which reported concentrations in mg/L with a precision of 0.001 mg/L following methods described by Smith et al. (2021) and Anderson et al. (2023) at Florida International University. Because of analytical issues, the sample size for DOC concentration analysis was reduced for the spring and summer events ($n = 26$ for each season). We analyzed all samples collected in early autumn and late autumn for DOC concentration ($n = 100$ for each season).

We measured the fluorescent optical properties of filtered water samples ($n = 100$ for early autumn, late autumn,

and spring; $n = 97$ for summer) to understand the chemical composition of DOM. We examined samples using fluorescence excitation–emission matrices (EEMs) with a fluorometer (Horiba Aqualog 2; Horiba®, Kyoto, Japan) at Florida International University. We measured EEMs at room temperature (~21°C) in a 1-cm quartz cuvette and simultaneously recorded fluorescence emission spectra from 212.719 to 620.797 nm in increments of 1.64 nm with an integration time of 2 s. We removed excitation wavelengths below 260 nm or above 500 nm and emission wavelengths below 280 nm or above 530 nm from the analysis to remove light scattering effects. For processing of EEM spectra, we used the DrEEM toolbox (version 6.1; Murphy et al. 2013) in MATLAB® (version R2022a; Mathworks®, Natick, Massachusetts) for instrument correction, inner-filter correction, blank correction, and Raman normalization (McKnight et al. 2001, Cory and McKnight 2005). We calculated fluorescence indices to assess the DOM composition, as described in Table 1. The fluorescence index (FI; Cory and McKnight 2005) provided insights into terrestrial and microbial sources, the humification index (HIX; Ohno 2002) explained humification and decomposition, and the biological index (BIX) offered information on autotrophic

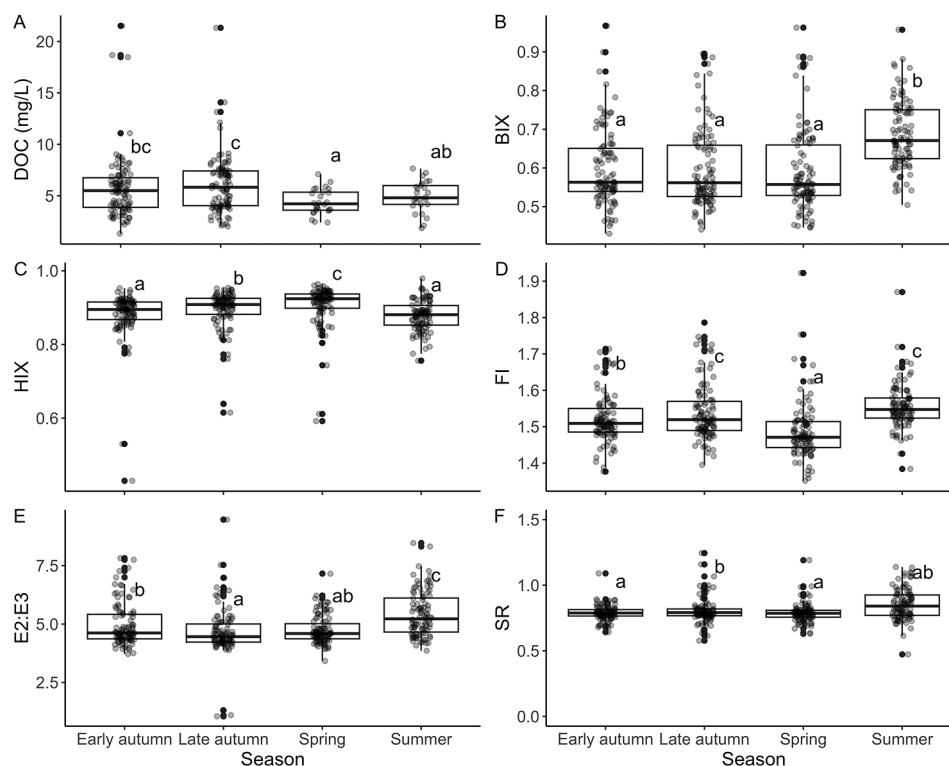


Figure 3. Dissolved organic C (DOC) concentration (A) and dissolved organic matter optical properties (described in Table 1) (B–F) for each sampling period (early autumn = September 2021, late autumn = November 2021, spring = April 2022, summer = July 2022). The $n = 100$ for all seasons and parameters, except $n = 26$ for DOC concentration in spring and summer. BIX = biological index (B), HIX = humification index (C), FI = fluorescence index (D), E2:E3 = ratio of absorbance at 250 nm to absorbance at 365 nm (E), SR = slope ratio (F). The 2 sites with very low HIX values in panel C are sites 49 and 50 (shown in Fig. 1C). Seasons with different lowercase letters differed, as determined by Tukey's honestly significant difference pairwise post-hoc test with $p \leq 0.05$.

production quality (Hansen et al. 2016). The natural log of the slope of absorbance spectra in 2 wavelength ranges ($S_{275-295}$, $S_{350-400}$) yielded the spectral slope ratio (SR). SR and absorption spectral slopes can be indicators of molecular weight and photochemical processing of chromophoric DOM (Helms et al. 2008). The absorption ratio between 250 and 365 nm (E2:E3) provides information about the DOM molecular size (De Haan and De Boer 1987).

Parallel factor analysis methods

Absorbing and fluorescing properties of CDOM have been used to fingerprint organic C sources, and often to track terrestrial DOM fluxes into the ocean (Coble 2007). We subjected the corrected EEM spectra from the samples collected in this study (~400), together with ~3410 additional samples from urban streams in Atlanta, Georgia, and Miami, Florida, USA, collected as part of a larger project examining urban influences on stream organic matter, to PARAFAC modeling using the DrEEM toolbox in MATLAB (Murphy et al. 2013) to distinguish overlapping fluorophores in the EEMs as individual components identified by their excitation and emission peaks. We chose the final 5-component model based on split-half analysis by S4C4T3 (Split -4, Combination -4, Test -3) validation (Fig. S1) as described in the appendix of Murphy et al. (2013) and the Fig. S2 caption.

Data analysis

To assess how characteristics of DOM varied among seasons (question 1), we used mixed-effects ANOVA with the `lmer` function from the `lme4` package in R (version 1.1-37; Bates et al. 2015), with season as a fixed effect and site and watershed as random effects. We used the `lmerTest` package (version 3.1-3; Kuznetsova et al. 2017) to extract Type III ANOVA tables for fixed effects and Tukey's honestly significant difference pairwise tests to compare seasonal variance of DOM characteristics, including DOC concentration, fluorescence indices BIX, FI, HIX, SR and E2:E3, and the relative contribution of the 5 PARAFAC components (% C1, % C2, % C3, % C4, and % C5). DOC concentration, % C4, and % C5 were natural log transformed to achieve normality, and all other variables were approximately normal. For all tests, linear relationships were visually assessed with scatterplots, and homoscedasticity was visually assessed by plotting residuals against predicted values.

To assess how watershed characteristics affect DOM characteristics (question 2), we used both principal component analysis (PCA) and linear mixed-effects models. First, to reduce the complexity and number of DOM characteristics, we conducted a PCA. We scaled DOM-characteristic data (FI, BIX, HIX, $S_{275-295}$, $S_{350-400}$, SR, E2:E3, % C1, % C2, % C3, % C4, and % C5) and conducted the PCA with the `prcomp` function from the `stats` package in R. We selected

Table 2. Excitation–emission (Ex/Em) spectra of 5 fluorescence components (C1–C5) identified by parallel factor analysis (PARAFAC) modeling compared with previously published similar PARAFAC components from the OpenFluor database (<https://openfluor.lablicate.com/>; Murphy et al. 2014), using a minimum similarity score of 0.90. Component 1 (C1) contained Ex/Em maxima at <250 nm and 300/396 nm, describing microbial humic-like dissolved organic matter (DOM) (Murphy et al. 2011, Lambert et al. 2016, Zhou et al. 2019). Component 2 (C2) was characterized by Ex/Em maxima at <250 nm and 396/488 nm, and the spectral Ex/Em maxima of component 3 (C3) were 261 nm and 399/455 nm. Both C2 and C3 resembled terrestrial humic-like fluorophores (Osburn et al. 2011, Lambert et al. 2016, Romero et al. 2017, Zhou et al. 2019, Retelletti Brogi et al. 2020, Zhuang et al. 2021). Component 4 (C4) had peak fluorescence (Ex/Em = 279/377 nm) in a region analogous to proteins and tryptophan-like DOM (Murphy et al. 2011, Zhou et al. 2019, Retelletti Brogi et al. 2020). Component 5 (C5) had 1 Ex maximum at 255 nm and 1 Em maximum at 321 nm, which overlapped benzoic acid-like DOM or monolignol-like DOM (D'Andrilli et al. 2017, Romero et al. 2017, Zhuang et al. 2021), suggesting fresh lignin-like precursors with low humic content but high bioavailability.

Component	Peak excitation wavelength (λ_{ex})/emission wavelength (λ_{em}) (nm)	Description	Similar components characterized in other studies
C1	<250, 300/396	Microbial, humic-like DOM	C2 (Lambert et al. 2016); G2 (Murphy et al. 2011); C4 (Zhou et al. 2019)
C2	<250, 396/488	Terrestrial, humic-like DOM	C2 (Zhuang et al. 2021); C2 (Romero et al. 2017); C2 (Retelletti Brogi et al. 2020)
C3	261, 339/445	Terrestrial, humic-like DOM	C1 (Osburn et al. 2011); C3 (Lambert et al. 2016); C1 (Zhou et al. 2019)
C4	279/377	Protein-like, tryptophan-like DOM	G5 (Murphy et al. 2011); C4 (Retelletti Brogi et al. 2020); C5 (Zhou et al. 2019)
C5	255/321	Fresh, lignin-like DOM	C4 (Zhuang et al. 2021); C1 (D'Andrilli et al. 2017); Benzoic acid (Wünsch et al. 2015)

principal components (PCs) with eigenvalues >1 for further analysis. We used variable loadings and visualizations to interpret the PCs. The first 3 PCs that explained the most variation were then used to characterize DOM composition and assess DOM variation with watershed characteristics.

We then used linear mixed-effects models and model selection using Akaike's information criterion (AIC) to identify the combination of watershed characteristics that was most associated with each PC. Predictor and response variables were assessed for normality and transformed as needed to improve normality (transformations are noted in the results). Linear relationships were visually assessed using scatterplots, and homoscedasticity was visually assessed by plotting residuals against predicted values. To account for repeated measures, we include site and watershed as random effects in all models. We proceeded with model selection in a stepwise manner. First, we compared linear mixed-effects models for each of the 3 PCs and all 17 individual watershed characteristics (variables described in Table S2; Spearman's correlation coefficients shown in Fig. S3). We included season as a fixed effect in these models and compared models with AIC and

marginal R^2 values. We then identified a best-fit model for each PC using stepwise model selection. We started by building an initial model for each PC that included all non-correlated predictors, as well as random effects of site and watershed. For correlated predictor variables (defined as $\rho > 0.4$; Table S2, Fig. S4), we chose the variable with a stronger association with the dependent variable. The best model for each PC was selected using the step function in R, and random effects were retained for all models. Because 2 of our watershed characteristics (housing age and % owner occupied) were not available for all sites (and thus made AICs incomparable), we ran model selection without these models and then compared the selected model with and without housing age and % owner occupied added back in.

RESULTS

DOM characteristics across sampling events

Precipitation patterns varied across the year, with conditions much wetter than normal (257% of mean monthly precipitation based on 2006–2020 data) during the early

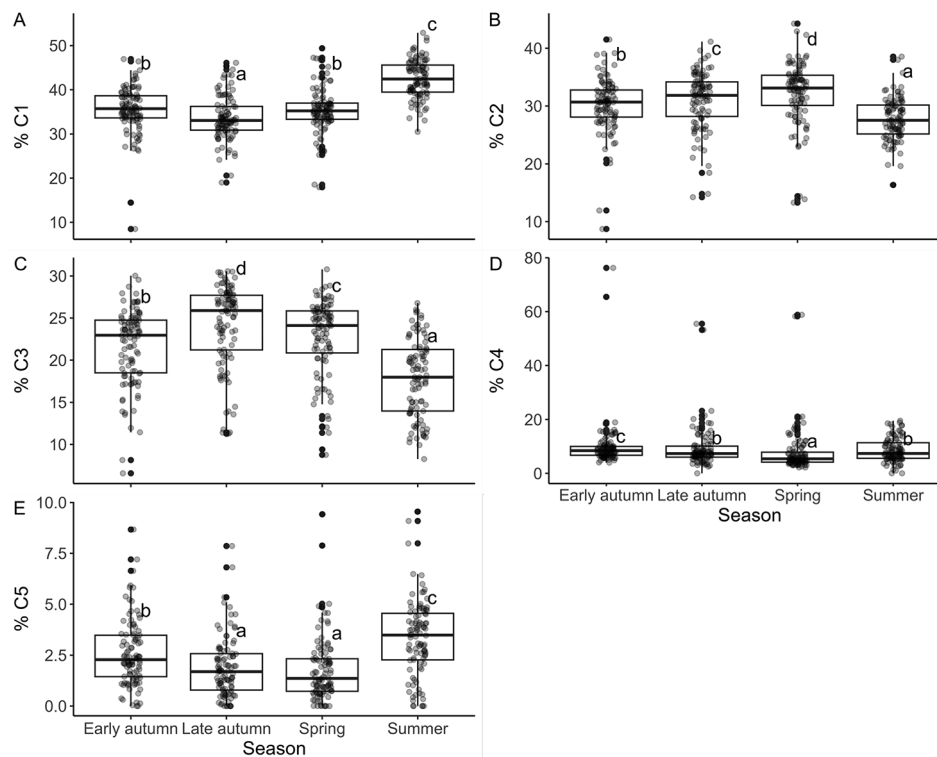


Figure 4. Percentages of the 5 dissolved organic matter (DOM) components (% C1–% C5) identified by parallel factor analysis modeling (based on ~3800 samples from this study area and 2 other urban areas using the same collection methods; see Table 2 for descriptions) for each sampling period (early autumn = September 2021, late autumn = November 2021, spring = April 2022, summer = July 2022). The 2 sites with high % C4 are sites 49 and 50 (shown in Fig. 1C). Seasons with different lowercase letters differed, as determined by Tukey's honestly significant difference pairwise post-hoc tests with $p \leq 0.05$. C1 = microbial, humic-like DOM (A), C2 = soil-derived terrestrial, humic-like DOM (B), C3 = plant-derived terrestrial, humic-like DOM (C), C4 = protein-like DOM (D), C5 = fresh, lignin-like DOM (E).

autumn (September 2021) sampling event, and conditions much drier than normal for the area (16% of mean precipitation) during the summer (July 2022) sampling event (NOAA 2024; see Table S1). DOC concentrations and DOM optical indices (described in Table 1) varied among some of the 4 synoptic sampling events (Tables S3, S4, Fig. 3A–F), corresponding to variability in precipitation and discharge among sampling events (Fig. 2). DOC concentrations were higher in late autumn than in the spring ($n = 100$ for each season; Table S4, Fig. 3A), though it should be noted that analytical issues resulted in a smaller sample size for DOC concentrations for the spring and summer events ($n = 26$ for each season; these analytical issues did not affect the fDOM samples used for PARAFAC modeling). Among the seasons, the dry summer synoptic event was the most distinct, showing higher BIX (reflecting more recent, autochthonous production; Fig. 3B), higher E2:E3 (lower molecular weight; Fig. 3E), and lower HIX (less humic; Fig. 3C) compared with other seasons. The spring samples had distinctly lower FI (Fig. 3D), indicative of a more-terrestrial, less-microbial source of DOM. Sites 49 and 50 (downstream of CSOs on Alewife Brook; Fig. 1C), had exceptionally low HIX values for all but the dry summer sampling event.

PARAFAC analysis resulted in 5 DOM components, based on EEMs (Table 2). Based on previous work, these components represent different types or characteristics of DOM. As with the fluorescence indices, PARAFAC components varied among seasons (Tables S3, S4, Fig. 4A–E). The dry summer sampling event was most distinctive, having higher percentages of C1 (microbial, humic-like; Table S4, Fig. 4A) and C5 (fresh, lignin-like; Fig. 4E) and lower percentages of C2 (soil-derived terrestrial, humic-like; Fig. 4B) and C3 (plant-derived terrestrial, humic-like; Fig. 4C) DOM. The percentage of C4 (protein-like) DOM was low (<20%) across all samples and seasons (Fig. 4D) except for sites 49 and 50. In Alewife Brook, % C4 increased 2- to 5-fold between 1 site upstream (site 51) and 2 sites downstream (sites 49 and 50) of CSO outfalls, but only during the wetter seasons when there were CSO events (Figs S5–S7).

In the PCA, the first 3 principal components of the DOM characteristics had eigenvalues >1 and cumulatively explained 85% of the variation in DOM characteristics (Table S5, Fig. 5A, B). PC1 explained >½ (52%) of the variation in DOM characteristics across the dataset, and it represented a gradient from more-microbial and autochthonous, lower-molecular-weight DOM (higher values of BIX and FI, lower E2:E3) to more-humic and terrestrial DOM (higher values of HIX, % C2, % C3). PC2 explained 20% of the variation in DOM characteristics. Higher values of PC2 had higher values of SR and $S_{350-400}$, which other studies (Blough and Del Vecchio 2002, Helms et al. 2008) have associated with lower molecular weights and photobleaching (Table 1). PC3 explained 13% of the DOM characteristics, reflecting a gradient from higher PARAFAC component C1 (microbial, humic-

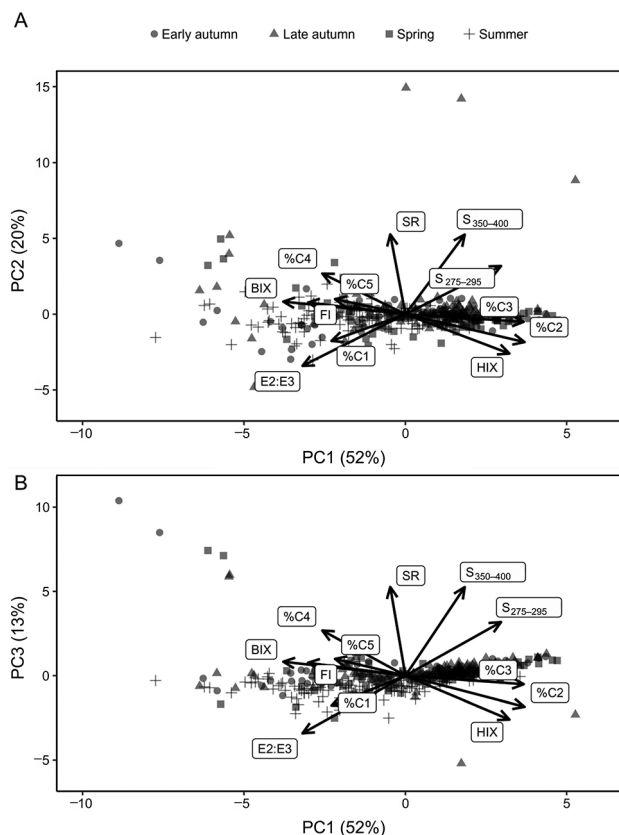


Figure 5. Principal component analysis of dissolved organic matter (DOM) characteristics for stream samples across seasons (symbols), with explanatory power shown for each of 3 principal components (PC1, PC2, and PC3): PC1 and PC2 (A) and PC1 and PC3 (B). PC1 represents a gradient from more-microbial and autochthonous DOM to more humic-like and allochthonous DOM. Higher values in PC2 reflect lower molecular weights and photobleaching (high SR and $S_{350-400}$). For PC3, low values reflect a higher % C1 (microbial humic-like DOM), and high values reflect higher % C4 (protein-like DOM). BIX = biological index, HIX = humification index, FI = fluorescence index, E2:E3 = ratio of absorbance at 250 nm to absorbance at 365 nm, SR = slope ratio, $S_{275-295}$ = nonlinear slope of absorbance from 275 to 295 nm, $S_{350-400}$ = nonlinear slope of absorbance from 350 to 400 nm.

like DOM) values to higher component C4 (protein-like DOM) values, likely driven by contributions from CSOs, as explained in the Discussion.

Watershed characteristics and DOM variability

Based on the single-predictor models that included the variation explained by season, PC1 was most highly correlated with % wetland cover (marginal $R^2 = 0.58$, conditional $R^2 = 0.82$; Table 3), indicating that watersheds with more wetland cover had more humic-like and allochthonous DOM in their streams (Fig. 6A). PC2 was not well correlated with any single watershed variable (Tables 3, S6),

Table 3. Summary statistics for watershed characteristics and results from the top single-predictor linear mixed-effects models between each watershed characteristic and principal component (PC1, PC2, PC3; PCs represent gradients in dissolved organic matter optical properties and parallel factor analysis components; Table S5). Fixed effects include single watershed predictor variable and season, and random effects include site and watershed. Data are from 100 stream sites sampled 4× over 1 y (September 2021, November 2021, April 2022, and July 2022) in the greater Boston, Massachusetts, USA, area. Models were compared using marginal R^2 (i.e., variation explained by the fixed effect only), and models for each PC are listed in order of increasing Akaike information criterion (AIC) value. The highest marginal R^2 value for predictor variable is in bold. DOM = dissolved organic matter, CSO = combined sewer overflow, MG = millions of gallons (1 MG = 3.8 million L³). See Table S6 for full modeling results for all watershed characteristics. A dash (–) indicates not applicable.

PC1								
High values = more-humic DOM, low values = more-microbial/autochthonous DOM								
Predictor variable	Model intercept	Intercept p	Predictor coefficient	Predictor p	Marginal R^2	Conditional R^2	Model AIC	Δ AIC
Housing age (y)	–4.30	0.0004	0.09	<0.0001	0.33	0.83	1309.70	0.00
Wetland (%)	–2.33	<0.0001	0.23	<0.0001	0.58	0.82	1369.76	60.06
Season alone	–0.17	0.8	–	–	0.13	0.84	1439.97	130.27
PC2								
High values = lower-molecular-weight/photobleached DOM, low values = higher-molecular-weight DOM								
Housing age (y)	0.38	0.4	–0.01	0.3	0.05	0.38	1203.92	0.00
Owner-occupied housing (%)	0.76	0.1	–1.16	0.08	0.06	0.31	1410.96	207.04
CSO density (no./km ²) ⁽⁴⁾	–0.17	0.3	1.68	0.005	0.08	0.31	1414.62	210.70
Season alone	–0.07	0.7	–	–	0.05	0.31	1421.44	217.52
PC3								
High values = lower-molecular-weight/photobleached DOM, low values = higher-molecular-weight DOM								
Housing age (y)	1.09	0.02	–0.01	0.07	0.14	0.66	999.96	0.00
30-d CSO flows (MG/km ²) ⁽⁴⁾	0.13	0.2	4.37	<0.0001	0.22	0.66	1014.10	14.14
CSO density (no./km ²) ⁽⁴⁾	0.10	0.4	3.28	<0.0001	0.30	0.65	1055.18	55.22
Season alone	0.31	0.1	–	–	0.10	0.65	1091.25	91.29

though CSO outfall density explained the most variation (marginal $R^2 = 0.08$, conditional $R^2 = 0.31$; Fig. 6B). The best single variable predictor for PC3 was also CSO outfall density (marginal $R^2 = 0.30$, conditional $R^2 = 0.65$; Fig. 6C). Housing age had the lowest AIC for all PC models (Table 3), but these low AIC scores were due to smaller sample size, and the explanatory power of housing age was comparatively low for all PCs.

Best-fit mixed-effects multiple linear regression models for each of the DOM characteristics PCs varied in predictors and overall explanatory power (Table 4). PC1 was the best predicted by watershed characteristics (marginal $R^2 = 0.68$, conditional $R^2 = 0.83$), compared with PC2 (marginal $R^2 = 0.13$, conditional $R^2 = 0.32$) and PC3 (marginal $R^2 = 0.36$, conditional $R^2 = 0.65$). PC1 (higher values associated with humic-like DOM, lower values associated with microbial and autochthonous DOM) values were positively associated with % wetland cover and median housing

age and negatively associated with % low income and CSO density. PC2, which described a gradient of low molecular weight (high values of PC2) to high molecular weight (low values of PC2), was positively associated with elevation and CSO density and negatively associated with % watershed canopy cover. PC3, which described a gradient of higher protein-like DOM to microbial, humic-like DOM, was positively associated with % wetland cover and CSO density.

DISCUSSION

This research expands on previous urban stream studies by incorporating sociodemographic, infrastructure, and infrastructure management variables to identify which aspects of development contribute to DOM properties and how these drivers change with temporal variation in inputs and hydrologic connectivity. We found that decreased connectivity to wetlands and terrestrial sources during dry periods is likely the strongest temporal control on DOM quantity and

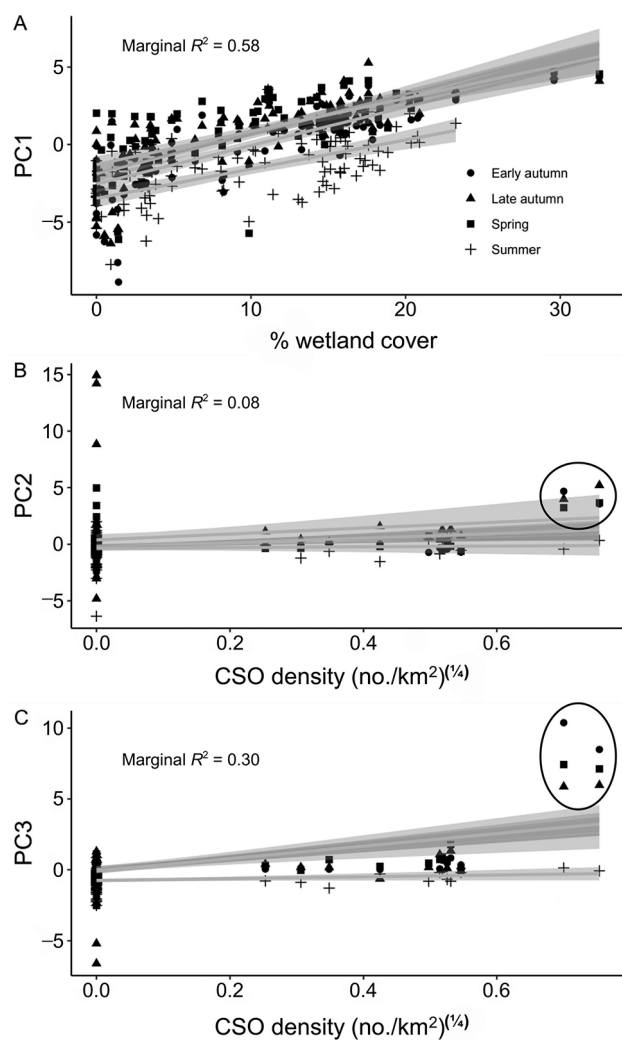


Figure 6. Single-predictor linear regression models, controlling for season, showing the best watershed predictors for each principal component (PC) based on marginal R^2 (see Tables 3 and 4): % wetland cover in the watershed vs PC1 (A), 4th root of combined sewer overflow (CSO) outfall density (no./km²) vs PC2 (B), and 4th root of CSO outfall density (no./km²) vs PC3 (C). The circled symbols in panels B and C show values at sites 49 and 50 in early autumn, late autumn, and spring (see Fig. 1C). PCs represent gradients in dissolved organic matter optical properties and absorbing and fluorescing properties determined by parallel factor analysis (Table S5).

characteristics. In the Boston metropolitan area, increased impervious cover and decreased wetland cover resulted in stream DOM that was more autotrophic, had lower molecular weight, and was likely more bioavailable. During higher flow conditions, CSOs introduced a large amount of protein-like DOM in streams with active outfalls (Figs S5, S7).

Seasonal variation in DOM

Our interpretations of seasonal effects on urban stream DOM are somewhat limited because our samples were not

all collected during baseflow conditions. In other studies, DOC concentration and humic DOM characteristics were elevated in samples collected during the rising limb of storm hydrographs (Inamdar et al. 2011, Raymond et al. 2016, Chen et al. 2019). Because we cannot be certain when each sample was collected on its respective stream hydrograph, our interpretations about seasonal shifts in DOM sources are limited to generalizations about wet and dry conditions and the approximate timing of events such as leaf fall.

In the autumn and spring, stream DOM was predominantly terrestrially sourced (higher HIX, % C2, and % C3; lower BIX, FI), likely from soil and groundwater DOM pools or possibly from leaf litter directly deposited on the stream or flushed through stormwater systems (Smith et al. 2021). Compared with the autumn and spring, DOM in the summer was derived from more-autotrophic, microbial sources (higher BIX, FI, and % C1) with lower molecular weight (higher E2:E3), possibly because of higher rates of instream photosynthesis associated with warmer temperatures and more hours of daylight (Arango et al. 2017).

The observed seasonal shifts in DOM characteristics are likely related to changes in streamflow and hydrologic connectivity. Our early autumn (September 2021) sampling event took place under unusually wet conditions, which can increase connectivity to terrestrial sources, including wetlands (Zarnetske et al. 2018, Leibowitz et al. 2019) and upslope areas (Stieglitz et al. 2003), and increase discharge from distributed stormwater systems. Such connectivity may be responsible for larger DOM fluxes (Zarnetske et al. 2018) and more-humic and aromatic DOM during high discharge events (Raymond et al. 2016). In contrast, our summer (July 2022) sampling took place during dry conditions. Under these low-flow conditions, contributions of terrestrial sources via connectivity to wetlands, upslope areas, and stormwater likely decreased. Relatively lower allochthonous contributions would help explain why the characteristics of the autochthonous DOM (higher BIX, FI, and % C1) were more prevalent in the samples collected during the dry summer season, consistent with other observations (Xenopoulos et al. 2021).

Watershed characteristics and DOM

Our results are largely consistent with previous observations (e.g., Kaushal et al. 2014, Parr et al. 2015) of the effects of urbanization: decreased DOC concentrations (Fig. S8) and more-autochthonous, recently produced, lower-molecular-weight, microbial DOM (Fig. S9). Distinct observations from this study include the substantial role of wetland loss in shifting DOM sources, clear CSO markers, and the observed influence of sociodemographic variables.

DOC concentrations were most strongly positively correlated with % wetland cover (Fig. S8) for all seasons except the dry summer (when streams were likely hydrologically disconnected from wetlands), suggesting that the draining of wetlands for development in the Boston area has resulted

Table 4. Best mixed-effects multiple regression models for each principal component (PC1, PC2, PC3; PCs represent gradients in dissolved organic material (DOM) optical properties and parallel factor analysis components; Table S5) as determined by highest marginal R^2 (fixed effects alone). Random effects of site and river were included in all models. Data are from 100 stream sites sampled 4× over 1 y (September 2021, November 2021, April 2022, and July 2022) in the greater Boston, Massachusetts, USA, area. A dash (–) indicates a single predictor, for which a parameter does not apply. MW = molecular weight.

	Model parameter	Coefficient	Coefficient p	Marginal R^2	Conditional R^2	AIC
PC1	Intercept	–0.54	0.57	0.68	0.83	1240.33
High values = more humic-like DOM, low values = microbial/autochthonous-like DOM	% wetland cover	0.16	<0.0001	–	–	–
	% low income	–0.87	<0.0001	–	–	–
	Housing age	0.03	0.03	–	–	–
	CSO density	–3.48	<0.0001	–	–	–
	Late autumn	0.79	<0.0001	–	–	–
	Spring	0.91	<0.0001	–	–	–
	Summer	–1.56	<0.0001	–	–	–
PC2	Intercept	–0.39	0.3	0.13	0.32	1421.63
High values = lower MW/ photobleached, low values = higher MW	% watershed canopy cover	–0.02	0.02	–	–	–
	Elevation	0.02	0.0003	–	–	–
	CSO density	1.72	<0.001	–	–	–
	Late autumn	0.61	0.001	–	–	–
	Spring	–0.08	0.7	–	–	–
	Summer	–0.30	0.10	–	–	–
PC3	Intercept	–0.34	0.03	0.36	0.65	1049.46
High values = protein-like DOM, low values = microbial, humic-like DOM	% wetland cover	0.04	<0.001	–	–	–
	CSO density	3.79	<0.0001	–	–	–
	Late autumn	–0.09	0.4	–	–	–
	Spring	–0.12	0.2	–	–	–
	Summer	–0.99	<0.0001	–	–	–

in lower DOC concentrations in the most urbanized watersheds. This finding is consistent with previous research showing wetlands as important DOM sources to freshwater systems (Findlay 2006, Flint and McDowell 2015, Zarnetske et al. 2018). Wetlands were also the strongest predictor of humic and allochthonous DOM (PC1; Figs 6 and S10, which are generalized in Fig. 7 using the slopes from mixed-effects models as shown in Table S7). The relationship between wetlands and DOM may be most pronounced in metropolitan areas like Boston, where much of the development has taken the place of wetlands (Rhodes et al. 2019, Zou et al. 2024). The draining of wetlands for urban development is associated with stream channelization, which decreases groundwater–surface-water connections (Kaushal et al. 2014), helping to explain the decrease in wetland and soil-derived (% C2 and % C3) humic components in developed watersheds. Other studies have reported that legacy humic organic matter in areas that have been recently developed may continue to contribute to streams, but that this contribution decreases over time (Petroni et al. 2011). These studies and our results suggest that the impacts of urbanization on stream

DOM may be shaped by linkages between predevelopment physiographic conditions (e.g., Boston is characterized by a low-relief landscape with numerous wetlands) and the characteristics and timing of human development. These linkages vary with hydrology because of variable connectivity to DOM sources (e.g., soils and wetlands) (Leibowitz et al. 2019). Because of the multiple physical and human factors that vary across cities (Walsh et al. 2005), it is important to consider the underlying landscape and developmental history when assessing potential C sources and transport in urban settings.

A key observation of this study is that protein-like DOM (C4) was likely an indicator of wastewater introduced by CSOs and wastewater treatment plants. Our synoptic samples above and below CSO outfalls in Alewife Brook highlighted the effect of CSO events in the wetter seasons (Figs S5 and S7A–C). A site downstream of a small wastewater treatment plant in the upper Charles River watershed showed elevated % C4 throughout the year, possibly due to consistent wastewater effluent inputs. Notably, % C4 was not elevated at the site upstream of the plant (Fig. S7A–D). Although

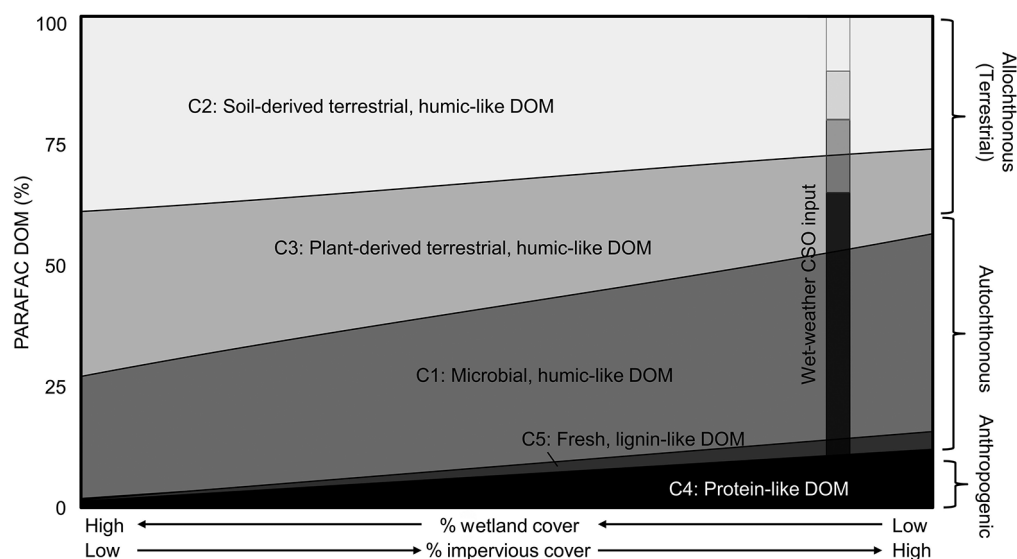


Figure 7. Synthesis of general patterns of relative stream dissolved organic matter (DOM) sources, based on parallel factor analysis (PARAFAC) components, across a gradient of wetland and impervious cover. The semitransparent vertical bar shows relative DOM contributions during wet weather when combined sewer overflow (CSO) inputs dominate an urban stream. Slopes for mixed-effects models of % PARAFAC components vs % wetland cover (Fig. S10) were calculated (excluding the 2 CSO-dominated sampling locations; Table S7) and used to draw lines for this figure. The maximum % wetland cover was 33% and the minimum was 0%. The gradient from low to high % impervious cover only indicates a general inverse relationship with % wetland cover in this study area (Spearman's $\rho = -0.77$).

protein-like DOM may come from many sources, including wastewater, algae, and microbes (Liao et al. 2021, Zhu et al. 2021), the evidence suggests that in Boston, % C4 may be used as a tracer for sewage inputs, as also suggested by other studies that associate protein-like DOM with wastewater (Hosen et al. 2014, Batista-Andrade et al. 2023) and wastewater indicators such as *Escherichia coli* (e.g., Smith et al. 2021). In urban areas that still have CSOs, wastewater discharge to streams may increase as climate change is expected to increase the intensity of storms (Gogien et al. 2023), which may be marked by increases in protein-like DOM in streams.

This study also offered an opportunity to investigate how sociodemographic factors may help explain DOM characteristics. Older housing was associated with more-humic and higher-molecular-weight DOM (Table 4), which may be explained by the higher wetland cover, lower impervious cover, and more canopy cover in areas with older housing compared with newer developments (e.g., Lowry et al. 2012, and data from this study; Fig. S4). Interestingly, housing age was weakly negatively correlated with % C4, which was counterintuitive given that housing age may be used as a proxy for infrastructure age (Weller et al. 2022) and wastewater leakage. Watersheds with higher % low-income populations were associated with more-microbial, autochthonous DOM. Lower-income communities may have less canopy cover and more impervious surfaces (e.g., Endsley et al. 2018, Culler et al. 2024, and spatial data from this study; Fig. S4), which could help explain the correlation be-

tween % low income and more-autochthonous DOM. However, none of the sociodemographic variables we examined had large predictor coefficients. The relationships between sociodemographic variables and DOM likely vary in strength and direction across cities, depending on their historical development patterns. Stronger relationships may emerge with alternative spatial classification schemes that combine physical and social characteristics (Cadenasso et al. 2007).

Broader implications

Our observations of varying DOM sources with urbanization and hydrological conditions have implications for stream-management priorities. DOM may influence stream metabolism, biochemical O_2 demand, and DO levels (McCabe et al. 2021, Zhou et al. 2021), and may also therefore influence the concentrations of chemical species of concern, such as NO_3^- , N_2O , and CO_2 , whose rates of production or consumption depend on DO levels and DOM availability (Quick et al. 2016). Contaminants may be sorbed to DOM (Kaushal et al. 2018, Al-Amin et al. 2024), which influences drinking water treatment (Findlay 2006, Gagliano et al. 2020, Leonard et al. 2022). It is therefore important for environmental agencies and water-quality managers to acknowledge shifts in DOM with urbanization.

Even though we observed that stream DOC concentrations decreased with urbanization (as generalized by impervious cover; Fig. S8), it is possible that DOM in urban areas is more bioavailable because it is more microbially produced

and has lower molecular weight (McLaughlin and Kaplan 2013, Catalán et al. 2021, Vaughn et al. 2023), as reported in other urban areas (Hosen et al. 2014, Parr et al. 2015, Smith et al. 2021, Coble et al. 2022, Vaughn et al. 2023). Increasing DOM bioavailability leads to higher rates of biogeochemical processing, including heterotrophic denitrification (Bernhardt and Likens 2002, Barnes et al. 2012) and increased NO_3^- removal, but also higher CO_2 emissions due to respiration (Hosen et al. 2014). Urbanization and its effects on CO_2 emissions from streams could be incorporated into plans for meeting greenhouse gas emissions targets for cities. The strong connection we observed between protein-like DOM (% C4) and CSOs suggests that water managers could incorporate similar markers to detect wastewater contamination from CSOs or failing infrastructure in need of repair. Combining DOM markers with sociodemographic data could be used to monitor the equitable prioritization of repairing wastewater infrastructure, closing CSOs, or restoring riparian vegetation. Although it was not a strong predictor, we did observe that more frequent street sweeping was associated with less-humic DOM in streams. Previous studies have examined the impact of street sweeping on N and P inputs (e.g., Bratt et al. 2017), but future studies are needed to better understand its impact on DOM, specifically organic C.

In examining temporal and spatial variability in DOM in urban streams, we observed the importance of novel anthropogenic sources (CSOs and wastewater), the alteration of wetland inputs due to urban development, and temporal variation in hydrologic connectivity. These factors are all subject to change as municipalities manage aging wastewater infrastructure systems and develop wetlands, and as climate change introduces uncertainty in hydrologic conditions. As demonstrated for the Boston metropolitan area, it is therefore critical to understand the drivers of stream DOM that are specific to a city's physiographic conditions and urban development characteristics.

ACKNOWLEDGEMENTS

Author contributions: RLH, AHR, and KGH conceived of this study as part of the larger Carbon in Urban River Biogeochemistry (CURB) effort. AMQ selected sampling sites in the Boston area. KGH delineated subwatersheds, compiled watershed spatial characteristics, and created hydrological figures. AMQ, RLH, AHR, SC, and LDOM designed field methods. AMQ and AHR conducted fieldwork. LDOM conducted laboratory analyses, and SC conducted PARAFAC modeling. RHL conducted statistical analyses. AMQ led the writing of the paper with contributions from all authors.

This work was supported by National Science Foundation Ecosystems awards 2015616, 2015619, 2015632, and 2015624, which funded the larger CURB project. Additional personnel on this project including co-principal investigators Krista Capps, John Kominoski, and Jen Morse, postdoctoral researcher Jacob Rudolph, graduate student Andrew Blinn, Smithsonian Environmental Research Center technicians Jessie Ribera and Carey Pelc, and Florida International University technician Christopher Rizzie all provided valuable con-

ceptual input, technical assistance, data management, and laboratory support. Undergraduate students at the University of Massachusetts Amherst (Jack Soucie, Andrew Wang, Ethan Risse, and Callista Macpherson) assisted with sample preparation and field work. The authors are also grateful for the assistance provided by the Charles River Watershed Association, Mystic River Watershed Association, and Neponset River Watershed Association in site selection, equipment storage, and recruiting field volunteers including John Monahan, Amanda Cantara, Gabrielle String, Sally Warner, Crystal Bowers, Lisa Troy, Mary Blanchette, and Yishen Li. We are very grateful to Thomas Parr (United States Geological Survey), *Freshwater Science* Editor-in-Chief Elizabeth Anderson, Associate Editor Nathan Smucker, Technical Editor Brooke Cassell, and 3 anonymous reviewers whose thorough reviews and comments greatly improved this manuscript.

Statements and declarations: The authors declare no conflicts of interest. Any use of trade, firm, or product names is for descriptive purposes only and does not imply endorsement by the United States Government.

Data availability: Data are available from the Environmental Data Initiative: <https://doi.org/10.6073/pasta/837f189bb5f6e3666f6c175a5bff082e>; <https://doi.org/10.6073/pasta/99b6ae080cad891c56175e0f6be93e62>; <https://doi.org/10.6073/pasta/715dd34e65f50366c8616859287f7d95>. Questions about the data may be directed to Annika Quick, aquick@vwu.edu.

LITERATURE CITED

- Al-Amin, A., R. J. Ryan, and E. R. McKenzie. 2024. Effects of dissolved organic carbon on potentially toxic element desorption in stormwater bioretention systems. *Science of the Total Environment* 912:168651.
- Allan, J. D., M. M. Castillo, and K. A. Capps. 2021. *Stream Ecology: Structure and function of running waters*. 3rd edition. Springer.
- Anderson, K. J., J. S. Kominoski, A. Nocentini, and S. Hoffman. 2023. Dissolved organic matter in peat and marl marshes varies with nutrient enrichment and restored hydrology. *Restoration Ecology* 31:e13905.
- Arango, C. P., J. J. Beaulieu, K. M. Fritz, B. H. Hill, C. M. Elonen, M. J. Pennino, P. M. Mayer, S. S. Kaushal, and A. D. Balz. 2017. Urban infrastructure influences dissolved organic matter quality and bacterial metabolism in an urban stream network. *Freshwater Biology* 62:1917–1928.
- Barnes, R. T., R. L. Smith, and G. R. Aiken. 2012. Linkages between denitrification and dissolved organic matter quality, Boulder Creek watershed, Colorado. *Journal of Geophysical Research: Biogeosciences* 117:G01014.
- Bates, D., M. Mächler, B. Bolker, and S. Walker. 2015. Fitting linear mixed-effects models using *lme4*. *Journal of Statistical Software* 67(1):1–48. (Available from <https://CRAN.R-project.org/package=lme4>)
- Batista-Andrade, J. A., E. Diaz, D. Iglesias Vega, E. Hain, M. R. Rose, and L. Blaney. 2023. Spatiotemporal analysis of fluorescent dissolved organic matter to identify the impacts of failing sewer infrastructure in urban streams. *Water Research* 229:119521.
- Batista-Andrade, J. A., C. Welty, D. Iglesias Vega, A. McClain, and L. Blaney. 2024. Geospatial variability of fluorescent dissolved organic matter in urban watersheds: Relationships with land cover and wastewater infrastructure. *Environmental Science & Technology* 58:7529–7542.

- Bernhardt, E. S., and G. E. Likens. 2002. Dissolved organic carbon enrichment alters nitrogen dynamics in a forest stream. *Ecology* 83:1689–1700.
- Bhaskar, A. S., K. G. Hopkins, B. K. Smith, T. A. Stephens, and A. J. Miller. 2020. Hydrologic signals and surprises in U.S. streamflow records during urbanization. *Water Resources Research* 56:e2019WR027039.
- Birch, W. S., M. Drescher, J. Pittman, and R. C. Rooney. 2022. Trends and predictors of wetland conversion in urbanizing environments. *Journal of Environmental Management* 310: 114723.
- Blough, N. V., and R. Del Vecchio. 2002. Chromophoric DOM in the coastal environment. Pages 509–546 in D. A. Hansell and C. A. Carlson (editors). *Biogeochemistry of marine dissolved organic matter*. Academic Press.
- Bratt, A. R., J. C. Finlay, S. E. Hobbie, B. D. Janke, A. C. Worm, and K. L. Kemmitt. 2017. Contribution of leaf litter to nutrient export during winter months in an urban residential watershed. *Environmental Science & Technology* 51:3138–3147.
- BWSC (Boston Water and Sewer Commission). 2024. Sewer system: History. (Available from <https://www.bwsc.org/environment-education/water-sewer-and-stormwater/sewer-system>, accessed March 2024)
- Cadenasso, M. L., S. T. A. Pickett, and K. Schwarz. 2007. Spatial heterogeneity in urban ecosystems: Reconceptualizing land cover and a framework for classification. *Frontiers in Ecology and the Environment* 5:80–88.
- Catalán, N., A. Pastor, C. M. Borrego, J. P. Casas-Ruiz, J. A. Hawkes, C. Gutiérrez, D. von Schiller, and R. Marcé. 2021. The relevance of environment vs. composition on dissolved organic matter degradation in freshwaters. *Limnology and Oceanography* 66:306–320.
- CDPW (Cambridge Department of Public Works). 2024. CSO activations. City of Cambridge, Cambridge, Massachusetts. (Available from <https://www.cambridgema.gov/Departments/publicworks/Initiatives/csoactivations>, accessed March 2024)
- Chen, S., Y. H. Lu, P. Dash, P. Das, J. Li, K. Capps, H. Majidzadeh, and M. Elliott. 2019. Hurricane pulses: Small watershed exports of dissolved nutrients and organic matter during large storms in the Southeastern USA. *Science of the Total Environment* 689:232–244.
- City of Somerville. 2024. Combined and sanitary sewer overflow control: CSO activation notifications. City of Somerville, Somerville, Massachusetts. (Available from <https://www.somervillema.gov/cso>, accessed March 2024)
- Coble, A. A., A. S. Wymore, J. D. Potter, and W. H. McDowell. 2022. Land use overrides stream order and season in driving dissolved organic matter dynamics throughout the year in a river network. *Environmental Science & Technology* 56:2009–2020.
- Coble, P. G. 2007. Marine optical biogeochemistry: The chemistry of ocean color. *Chemical Reviews* 107:402–418.
- Cory, R. M., and D. M. McKnight. 2005. Fluorescence spectroscopy reveals ubiquitous presence of oxidized and reduced quinones in dissolved organic matter. *Environmental Science & Technology* 39:8142–8149.
- Cory, R. M., M. P. Miller, D. M. McKnight, J. J. Guerard, and P. L. Miller. 2010. Effect of instrument-specific response on the analysis of fulvic acid fluorescence spectra. *Limnology and Oceanography: Methods* 8:67–78.
- Culler, M., J. Wickham, M. Nash, and M. T. Clement. 2024. Impervious cover change as an indicator of environmental equity. *Remote Sensing Applications: Society and Environment* 35:101247.
- D’Andrilli, J., C. M. Foreman, M. Sigl, J. C. Priscu, and J. R. McConnell. 2017. A 21 000-year record of fluorescent organic matter markers in the WAIS Divide ice core. *Climate of the Past* 13:533–544.
- De Haan, H., and T. De Boer. 1987. Applicability of light absorbance and fluorescence as measures of concentration and molecular size of dissolved organic carbon in humic Lake Tjeukemeer. *Water Research* 21:731–734.
- Dewitz, J. 2023. National Land Cover Database (NLCD) 2021 products: United States Geological Survey data release. (Available from <https://doi.org/10.5066/P9JZ7AO3>)
- Eckard, R. S., B. A. Pellerin, B. A. Bergamaschi, P. A. M. Bachand, S. M. Bachand, R. G. M. Spencer, and P. J. Hernes. 2017. Dissolved organic matter compositional change and biolability during two storm runoff events in a small agricultural watershed. *Journal of Geophysical Research: Biogeosciences* 122:2634–2650.
- Egea, L. G., F. G. Brun, and R. Jiménez-Ramos. 2024. Dissolved organic carbon leaching from microplastics and bioavailability in coastal ecosystems. *Science of the Total Environment* 909:168673.
- Endsley, K. A., D. G. Brown, and E. Bruch. 2018. Housing market activity is associated with disparities in urban and metropolitan vegetation. *Ecosystems* 21:1593–1607.
- Fellman, J. B., E. Hood, and R. G. M. Spencer. 2010. Fluorescence spectroscopy opens new windows into dissolved organic matter dynamics in freshwater ecosystems: A review. *Limnology and Oceanography* 55:2452–2462.
- Findlay, S. 2006. Dissolved organic matter. Pages 239–248 in F. R. Hauer and G. A. Lamberti (editors). *Methods in stream ecology*. 2nd edition. Academic Press.
- Flint, S. A., and W. H. McDowell. 2015. Effects of headwater wetlands on dissolved nitrogen and dissolved organic carbon concentrations in a suburban New Hampshire watershed. *Freshwater Science* 34:456–471.
- Forgrave, R., E. M. Elliott, and D. J. Bain. 2022. Event scale hydrograph responses highlight impacts of widespread stream burial and urban infrastructure failures. *Hydrological Processes* 36:e14584.
- Gagliano, E., M. Sgroi, P. P. Falciglia, F. G. A. Vagliasindi, and P. Roccaro. 2020. Removal of poly- and perfluoroalkyl substances (PFAS) from water by adsorption: Role of PFAS chain length, effect of organic matter and challenges in adsorbent regeneration. *Water Research* 171:115381.
- Gogien, F., M. Dechesne, R. Martinerie, and G. Lipeme Kouyi. 2023. Assessing the impact of climate change on Combined Sewer Overflows based on small time step future rainfall time-series and long-term continuous sewer network modelling. *Water Research* 230:119504.
- Graeber, D., Y. Tenzin, M. Stutter, G. Weigelhofer, T. Shatwell, W. von Tümpling, J. Tittel, A. Wachholz, and D. Borchardt. 2021. Bioavailable DOC: Reactive nutrient ratios control heterotrophic nutrient assimilation—An experimental proof of the macronutrient-access hypothesis. *Biogeochemistry* 155: 1–20.

- Griffith, D. R., R. T. Barnes, and P. A. Raymond. 2009. Inputs of fossil carbon from wastewater treatment plants to U.S. rivers and oceans. *Environmental Science & Technology* 43:5647–5651.
- Hancock, P. J. 2002. Human impacts on the stream–groundwater exchange zone. *Environmental Management* 29:763–781.
- Hansen, A. M., T. E. C. Kraus, B. A. Pellerin, J. A. Fleck, B. D. Downing, and B. A. Bergamaschi. 2016. Optical properties of dissolved organic matter (DOM): Effects of biological and photolytic degradation. *Limnology and Oceanography* 61:1015–1032.
- Hasenmueller, E. A., and H. K. Robinson. 2016. Hyporheic zone flow disruption from channel linings: Implications for the hydrology and geochemistry of an urban stream, St. Louis, Missouri, USA. *Journal of Earth Science* 27:98–109.
- Helms, J. R., A. Stubbins, J. D. Ritchie, E. C. Minor, D. J. Kieber, and K. Mopper. 2008. Absorption spectral slopes and slope ratios as indicators of molecular weight, source, and photo-bleaching of chromophoric dissolved organic matter. *Limnology and Oceanography* 53:955–969.
- Hopkins, K. G., and D. J. Bain. 2018. Research note: Mapping spatial patterns in sewer age, material, and proximity to surface waterways to infer sewer leakage hotspots. *Landscape and Urban Planning* 170:320–324.
- Hopkins, K. G., R. Hale, K. Capps, J. Kominoski, J. Morse, A. Roy, A. Blinn, S. Chen, L. Ortiz Muñoz, A. Quick, and J. Rudolph. 2024. Landscape characteristics for urban gradients in United States cities across multiple scales. United States Geological Survey data release. (Available from <https://doi.org/10.5066/P13UZYZF>)
- Hosen, J. D., O. T. McDonough, C. M. Febria, and M. A. Palmer. 2014. Dissolved organic matter quality and bioavailability changes across an urbanization gradient in headwater streams. *Environmental Science & Technology* 48:7817–7824.
- Inamdar, S., S. Singh, S. Dutta, D. Levia, M. Mitchell, D. Scott, H. Bais, and P. McHale. 2011. Fluorescence characteristics and sources of dissolved organic matter for stream water during storm events in a forested mid-Atlantic watershed. *Journal of Geophysical Research: Biogeosciences* 116:G03043.
- Johnson, L. R., T. L. E. Trammell, T. J. Bishop, J. Barth, S. Drzyzga, and C. Jantz. 2020. Squeezed from all sides: Urbanization, invasive species, and climate change threaten riparian forest buffers. *Sustainability* 12:1448.
- Kaushal, S. S., and K. T. Belt. 2012. The urban watershed continuum: Evolving spatial and temporal dimensions. *Urban Ecosystems* 15:409–435.
- Kaushal, S. S., K. Delaney-Newcomb, S. E. G. Findlay, T. A. Newcomer, S. Duan, M. J. Pennino, G. M. Svirichi, A. M. Sides-Raley, M. R. Walbridge, and K. T. Belt. 2014. Longitudinal patterns in carbon and nitrogen fluxes and stream metabolism along an urban watershed continuum. *Biogeochemistry* 121:23–44.
- Kaushal, S. S., A. J. Gold, S. Bernal, T. A. Newcomer Johnson, K. Addy, et al. 2018. Watershed ‘chemical cocktails’: Forming novel elemental combinations in Anthropocene fresh waters. *Biogeochemistry* 141:281–305.
- Kuznetsova, A., P. B. Brockhoff, and R. H. B. Christensen. 2017. *lmerTest* package: Tests in linear mixed effects models. *Journal of Statistical Software* 82(13):1–26.
- Lambert, T., C. R. Teodoru, F. C. Nyoni, S. Bouillon, F. Darchambeau, P. Massicotte, and A. V. Borges. 2016. Along-stream transport and transformation of dissolved organic matter in a large tropical river. *Biogeosciences* 13:2727–2741.
- Leibowitz, S. G., P. J. Wigington Jr, K. A. Schofield, L. C. Alexander, M. K. Vanderhoof, and H. E. Golden. 2019. Connectivity of streams and wetlands to downstream waters: An integrated systems framework. *Journal of the American Water Resources Association* 54:298–322.
- Leonard, L. T., G. F. Vanzin, V. A. Garayburu-Caruso, S. S. Lau, C. A. Beutler, A. W. Newman, W. A. Mitch, J. C. Stegen, K. H. Williams, and J. O. Sharp. 2022. Disinfection by products formed during drinking water treatment reveal an export control point for dissolved organic matter in a subalpine headwater stream. *Water Research X* 15:100144.
- Li, P., and J. Hur. 2017. Utilization of UV-Vis spectroscopy and related data analyses for dissolved organic matter (DOM) studies: A review. *Critical Reviews in Environmental Science and Technology* 47:131–154.
- Liao, Z.-L., Z.-C. Zhao, J.-C. Zhu, H. Chen, and D.-Z. Meng. 2021. Complexing characteristics between Cu(II) ions and dissolved organic matter in combined sewer overflows: Implications for the removal of heavy metals by enhanced coagulation. *Chemosphere* 265:129023.
- Lindsay, J. B. 2016. Whitebox GAT: A case study in geomorphometric analysis. *Computers & Geosciences* 95:75–84. (Available from <https://CRAN.R-project.org/package=whitebox>)
- Locke, D. H., B. Hall, J. M. Grove, S. T. A. Pickett, L. A. Ogdén, C. Aoki, C. G. Boone, and J. P. M. O’Neil-Dunne. 2021. Residential housing segregation and urban tree canopy in 37 US Cities. *npj Urban Sustainability* 1:15.
- Lowry Jr, J. H., M. E. Baker, and R. D. Ramsey. 2012. Determinants of urban tree canopy in residential neighborhoods: Household characteristics, urban form, and the geophysical landscape. *Urban Ecosystems* 15:247–266.
- McCabe, K. M., E. M. Smith, S. Q. Lang, C. L. Osburn, and C. R. Benitez-Nelson. 2021. Particulate and dissolved organic matter in stormwater runoff influences oxygen demand in urbanized headwater catchments. *Environmental Science & Technology* 55:952–961.
- McKnight, D. M., E. W. Boyer, P. K. Westerhoff, P. T. Doran, T. Kulbe, and D. T. Andersen. 2001. Spectrofluorometric characterization of dissolved organic matter for indication of precursor organic material and aromaticity. *Limnology and Oceanography* 46:38–48.
- McLaughlin, C., and L. A. Kaplan. 2013. Biological lability of dissolved organic carbon in stream water and contributing terrestrial sources. *Freshwater Science* 32:1219–1230.
- MEOEAA (Massachusetts Executive Office of Energy and Environmental Affairs). 2024. Sewage notification incidents. Massachusetts Executive Office of Energy and Environmental Affairs, Boston, Massachusetts. (Available from <https://eeaonline.eea.state.ma.us/portal/dep/cso-data-portal/>, accessed March 2024)
- Mostofa, K. M. G., C.-Q. Liu, D. Vione, M. A. Mottaleb, H. Ogawa, S. M. Tareq, and T. Yoshioka. 2013. Colored and chromophoric dissolved organic matter in natural waters. Pages 365–428 in K. M. G. Mostofa, T. Yoshioka, M. A. Mottaleb, and D. Vione (editors). *Photobiogeochemistry of organic matter: Principles and practices in water environments*. Springer.

- Murphy, K. R., A. Hambly, S. Singh, R. K. Henderson, A. Baker, R. Stuetz, and S. J. Khan. 2011. Organic matter fluorescence in municipal water recycling schemes: Toward a unified PARAFAC model. *Environmental Science & Technology* 45: 2909–2916.
- Murphy, K. R., C. A. Stedmon, D. Graeber, and R. Bro. 2013. Fluorescence spectroscopy and multi-way techniques. *PARAFAC. Analytical Methods* 5:6557–6566.
- Murphy, K. R., C. A. Stedmon, P. Wenig, and R. Bro. 2014. OpenFluor— An online spectral library of auto-fluorescence by organic compounds in the environment. *Analytical Methods* 6:658–661.
- MWRA (Massachusetts Water Resources Authority). 2022. CSO annual report: CSO discharge estimates and rainfall analyses for calendar year 2021. Massachusetts Water Resources Authority, Boston, Massachusetts. (Available from <http://ftp.mwra.com/cso/annualdischargeestimates.html>)
- MWRA (Massachusetts Water Resources Authority). 2024a. Combined sewer overflow (CSO) notifications. Massachusetts Water Resources Authority, Boston, Massachusetts. (Available from https://www.mwra.com/harbor/html/cso_reporting.htm, accessed March 2024)
- MWRA (Massachusetts Water Resources Authority). 2024b. Combined sewer overflows (CSOs). Massachusetts Water Resources Authority, Boston, Massachusetts. (Available from <https://www.mwra.com/03sewer/html/sewco.htm>, accessed March 2024)
- Mystic River Watershed Association. 2022. CSOs on the Mystic 2021. (Available from <https://mysticriver.org/news/2022/2/1/lh84chignvoj8mtx90ae5248031g3>)
- Napieralski, J., A. Guin, and C. Sulich. 2024. Buried but not dead: The impact of stream and wetland loss on flood risk in redlined neighborhoods. *City and Environment Interactions* 21:100134.
- Napieralski, J., R. Keeling, M. Dziekan, C. Rhodes, A. Kelly, and K. Kobberstad. 2015. Urban stream deserts as a consequence of excess stream burial in urban watersheds. *Annals of the Association of American Geographers* 105:649–664.
- NAWM (National Association of Wetland Managers). 2015. Massachusetts state wetland program summary. National Association of Wetland Managers, Portland, Maine. (Available from <https://www.nawm.aswm.org/wetland-programs/state-wetland-programs/state-program-summaries.html>)
- NOAA (National Oceanic and Atmospheric Administration). 2024. NOWData - NOAA Online weather data. Boston/Norton, Massachusetts Weather Forecast Office, Norton, Massachusetts. (Available from <https://www.weather.gov/wrh/Climate?wfo=box>, accessed March 2024)
- Ohno, T. 2002. Fluorescence inner-filtering correction for determining the humification index of dissolved organic matter. *Environmental Science & Technology* 36:742–746.
- Osburn, C. L., C. R. Wigdahl, S. C. Fritz, and J. E. Saros. 2011. Dissolved organic matter composition and photoreactivity in prairie lakes of the U.S. Great Plains. *Limnology and Oceanography* 56:2371–2390.
- Parr, T. B., C. S. Cronan, T. Ohno, S. E. G. Findlay, S. M. C. Smith, and K. S. Simon. 2015. Urbanization changes the composition and bioavailability of dissolved organic matter in headwater streams. *Limnology and Oceanography* 60:885–900.
- Parr, T. B., N. J. Smucker, C. N. Bentsen, and M. W. Neale. 2016. Potential roles of past, present, and future urbanization characteristics in producing varied stream responses. *Freshwater Science* 35:436–443.
- Petrone, K. C., J. B. Fellman, E. Hood, M. J. Donn, and P. F. Grierson. 2011. The origin and function of dissolved organic matter in agro-urban coastal streams. *Journal of Geophysical Research: Biogeosciences* 116:G01028.
- PRISM Climate Group. 2023. 30-year average annual values for 1991–2020. Oregon State University, Corvallis, Oregon. (Available from <https://prism.oregonstate.edu/>)
- Quick, A. M., W. J. Reeder, T. B. Farrell, D. Tonina, K. P. Feris, and S. G. Benner. 2016. Controls on nitrous oxide emissions from the hyporheic zones of streams. *Environmental Science & Technology* 50:11491–11500.
- Quick, A. M., A. H. Roy, and A. Wang. 2025. Field data for seasonal synoptic sampling of 100 urban streams in Boston, Massachusetts (USA) from 2021–2022 ver 1. Environmental Data Initiative, Madison, Wisconsin. (Available from <https://doi.org/10.6073/pasta/837f189bb5f6e3666f6c175a5bff082e>)
- Raymond, P. A., J. E. Saiers, and W. V. Sobczak. 2016. Hydrological and biogeochemical controls on watershed dissolved organic matter transport: Pulse-shunt concept. *Ecology* 97:5–16.
- Regnier, P., P. Friedlingstein, P. Ciais, F. T. Mackenzie, N. Gruber, et al. 2013. Anthropogenic perturbation of the carbon fluxes from land to ocean. *Nature Geoscience* 6:597–607.
- Retelletti Brogi, S., C. Balestra, R. Casotti, G. Cossarini, Y. Galletti, M. Gonnelli, S. Vestri, and C. Santinelli. 2020. Time resolved data unveils the complex DOM dynamics in a Mediterranean river. *Science of the Total Environment* 733:139212.
- Rhodes, L., M. McHugh, and T. Gruszkos. 2019. Inland and coastal wetlands of Massachusetts: Status and trends. Massachusetts Department of Environmental Protection, Boston, Massachusetts. (Available from <https://www.mass.gov/orgs/massachusetts-department-of-environmental-protection>)
- Roebuck Jr, J. A., M. Seidel, T. Dittmar, and R. Jaffé. 2020. Controls of land use and the river continuum concept on dissolved organic matter composition in an anthropogenically disturbed subtropical watershed. *Environmental Science & Technology* 54:195–206.
- Romero, C. M., R. E. Engel, J. D’Andrilli, C. Chen, C. Zabinski, P. R. Miller, and R. Wallander. 2017. Bulk optical characterization of dissolved organic matter from semiarid wheat-based cropping systems. *Geoderma* 306:40–49.
- Roy, A. H., A. L. Dybas, K. M. Fritz, and H. R. Lubbers. 2009. Urbanization affects the extent and hydrologic permanence of headwater streams in a midwestern US metropolitan area. *Journal of the North American Benthological Society* 28: 911–928.
- Roy, A. H., A. M. Quick, R. L. Hale, K. G. Hopkins, and J. S. Soucie. 2025. Salting behaviors influence urban stream conductivity in Boston, Massachusetts (USA). *Freshwater Science* 44:XX–XX.
- Smith, M. A., J. S. Kominoski, E. E. Gaiser, R. M. Price, and T. G. Troxler. 2021. Stormwater runoff and tidal flooding transform dissolved organic matter composition and increase bioavailability in urban coastal ecosystems. *Journal of Geophysical Research: Biogeosciences* 126:e2020JG006146.
- Sondergaard, M., and M. Middelboe. 1995. A cross-system analysis of labile dissolved organic carbon. *Marine Ecology Progress Series* 118:283–294.

- Stieglitz, M., J. Shaman, J. McNamara, V. Engel, J. Shanley, and G. W. Kling. 2003. An approach to understanding hydrologic connectivity on the hillslope and the implications for nutrient transport. *Global Biogeochemical Cycles* 17:1105.
- USCB (United States Census Bureau). 2010. Special release - Census blocks with population and housing counts. TIGER/Line shapefiles. United States Census Bureau, United States Department of Commerce, Washington, DC. (Available from <https://www.census.gov/geographies/mapping-files/2010/geo/tiger-line-file.html>)
- USEPA (United States Environmental Protection Agency). 2014. Enforcement and compliance history online. United States Environmental Protection Agency, Washington, DC. (Available from <https://echo.epa.gov/>, accessed July 2014)
- USEPA (United States Environmental Protection Agency). 2023a. EJScreen: Environmental justice screening and mapping tool. United States Environmental Protection Agency, Washington, DC. (Available from <https://www.epa.gov/system/files/documents/2024-07/ejscreen-tech-doc-version-2-3.pdf>, accessed August 2023)
- USEPA (United States Environmental Protection Agency). 2023b. History of human impacts on Charles River. United States Environmental Protection Agency, Washington, DC. (Available from <https://www.epa.gov/charlesriver/history-human-impacts-charles-river>)
- USGS (United States Geological Survey). 2021a. National Land Cover Database (NLCD) conterminous United States (CONUS) 2021 tree canopy cover. Version 2021-4. United States Geological Survey, Sioux Falls, South Dakota. (Available from https://www.mrlc.gov/downloads/sciweb1/shared/mrlc/meta_data/nlcd_tcc_conus_2021_v2021-4.tif.html)
- USGS (United States Geological Survey). 2021b. USGS 1/3 arc second n43w072 20211109. United States Geological Survey, Sioux Falls, South Dakota. (Available from <https://www.sciencebase.gov/catalog/item/61934907d34eb622f68e8655>, accessed February 2022)
- USGS (United States Geological Survey). 2023. National Hydrography Plus High Resolution National Release 1. United States Geological Survey, Sioux Falls, South Dakota. (Available from [https://prd-tnm.s3.amazonaws.com/index.html?prefix=Staged Products/Hydrography/NHDPlusHR/National/](https://prd-tnm.s3.amazonaws.com/index.html?prefix=Staged%20Products/Hydrography/NHDPlusHR/National/))
- Vaughn, D. R., A. M. Kellerman, K. P. Wickland, R. G. Striegl, D. C. Podgorski, J. R. Hawkings, J. H. Nienhuis, M. M. Dornblaser, E. G. Stets, and R. G. M. Spencer. 2023. Bioavailability of dissolved organic matter varies with anthropogenic landcover in the Upper Mississippi River Basin. *Water Research* 229:119357.
- Walker, K., and M. Herman. 2025. *tidycensus*: Load US census boundary and attribute data as 'tidyverse' and 'sf'-ready data frames. (Available from <https://CRAN.R-project.org/package=tidycensus>)
- Walsh, C. J., A. H. Roy, J. W. Feminella, P. D. Cottingham, P. M. Groffman, and R. P. Morgan II. 2005. The urban stream syndrome: Current knowledge and the search for a cure. *Journal of the North American Benthological Society* 24:706–723
- Weller, Z. D., S. Im, V. Palacios, E. Stuchiner, and J. C. von Fischer. 2022. Environmental injustices of leaks from urban natural gas distribution systems: Patterns among and within 13 U.S. metro areas. *Environmental Science & Technology* 56:8599–8609.
- Wu, Q., and A. Brown. 2022. *whitebox*: 'WhiteboxTools' R frontend. R package version 1.4.0/r27. (Available from <https://CRAN.R-project.org/package=whitebox>)
- Wünsch, U. J., K. R. Murphy, and C. A. Stedmon. 2015. Fluorescence quantum yields of natural organic matter and organic compounds: Implications for the fluorescence-based interpretation of organic matter composition. *Frontiers in Marine Science* 2:98.
- Xenopoulos, M. A., R. T. Barnes, K. S. Boodoo, D. Butman, N. Catalán, S. C. D'Amario, C. Fasching, D. N. Kothawala, O. Pisani, C. T. Solomon, R. G. M. Spencer, C. J. Williams, and H. F. Wilson. 2021. How humans alter dissolved organic matter composition in freshwater: Relevance for the Earth's biogeochemistry. *Biogeochemistry* 154:323–348.
- Zarnetske, J. P., M. Bouda, B. W. Abbott, J. Saiers, and P. A. Raymond. 2018. Generality of hydrologic transport limitation of watershed organic carbon flux across ecoregions of the United States. *Geophysical Research Letters* 45:11,702–11,711.
- Zhou, Y., P. Martin, and M. Müller. 2019. Composition and cycling of dissolved organic matter from tropical peatlands of coastal Sarawak, Borneo, revealed by fluorescence spectroscopy and parallel factor analysis. *Biogeosciences* 16:2733–2749.
- Zhou, Y., X. Yao, L. Zhou, Z. Zhao, X. Wang, K.-S. Jang, W. Tian, Y. Zhang, D. C. Podgorski, R. G. M. Spencer, D. N. Kothawala, E. Jeppesen, and F. Wu. 2021. How hydrology and anthropogenic activity influence the molecular composition and export of dissolved organic matter: Observations along a large river continuum. *Limnology and Oceanography* 66:1730–1742.
- Zhu, Q., X. Li, G. Li, W. Tang, C. Li, J. Li, C. Zhao, C. Du, X. Liang, W. Li, and L. Zhang. 2021. New insights into restoring microbial communities by side-stream supersaturated oxygenation to improve the resilience of rivers affected by combined sewer overflows. *Science of the Total Environment* 782:146903.
- Zhuang, W.-E., W. Chen, Q. Cheng, and L. Yang. 2021. Assessing the priming effect of dissolved organic matter from typical sources using fluorescence EEMs-PARAFAC. *Chemosphere* 264:128600.
- Zou, Z., C. Huang, M. W. Lang, L. Du, G. McCarty, J. C. Ingebritsen, J. Harner, R. Griffin, W. Gong, and J. Lu. 2024. Hotspots of wetland loss to impervious surfaces in the conterminous United States. *Science of the Total Environment* 948:174787.